

pubs.acs.org/Biomac Article

# Nanoscale Structure, Interactions, and Dynamics of Centromere Nucleosomes

Shaun Filliaux, Zhiqiang Sun, and Yuri L. Lyubchenko\*



Cite This: https://doi.org/10.1021/acs.biomac.3c01440



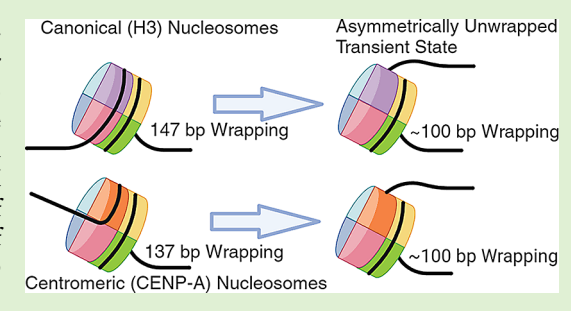
**ACCESS** I

III Metrics & More

Article Recommendations

SI Supporting Information

ABSTRACT: Centromeres are specific segments of chromosomes comprising two types of nucleosomes: canonical nucleosomes containing an octamer of H2A, H2B, H3, and H4 histones and CENP-A nucleosomes in which H3 is replaced with its analogue CENP-A. This modification leads to a difference in DNA wrapping (~121 bp), considerably less than 147 bp in canonical nucleosomes. We used atomic force microscopy (AFM) and high-speed AFM (HS-AFM) to characterize nanoscale features and dynamics for both types of nucleosomes. For both nucleosomes, spontaneous asymmetric unwrapping of DNA was observed, and this process occurs via a transient state with ~100 bp DNA wrapped around the core, followed by a rapid dissociation of DNA. Additionally, HS-AFM revealed higher stability of CENP-A nucleosomes



compared with H3 nucleosomes in which dissociation of the histone core occurs prior to the nucleosome dissociation. These results help elucidate the differences between these nucleosomes and the potential biological necessity for CENP-A nucleosomes.

# ■ INTRODUCTION

Nucleosomes are the fundamental nano assemblies in chromatin, the assembly of which is the first step for packing DNA in the nucleus.<sup>1,2</sup> Interaction between nucleosomes is a fundamental property that defines the assembly and function of chromatin. Studies over the past two decades have revealed highly dynamic features of nucleosomes that can explain regulatory processes at the chromatin level (e.g., see recent <sup>5</sup>). However, structural details and the mechanism underlying the assembly of nucleosomes in higher-order structures of chromatin and their dynamics remain unexplained. Many cellular processes, such as transcription, require the dissociation of DNA from nucleosomes, which is achieved through nucleosome dynamics and remodeling machinery.<sup>6</sup> Structural and single-molecule studies of these processes have been critical in developing current nucleosome models; however, the strong reliance on nucleosome positioning sequences for these techniques raises the question of how nucleosome structure and dynamics differ for those assembled on positioning vs nonpositioning DNA sequences. We used DNA templates with different sequences and AFM visualization to directly characterize the role of the DNA sequence on the positioning of nucleosomes and their interactions. 5,9–13 In paper, 13 we used DNA templates with different sequences and found that nucleosomes are capable of close positioning with no discernible space between them, even in the case of assembled dinucleosomes. This array morphology contrasts with that observed for arrays assembled with repeats of the nucleosome positioning motifs separated by uniform spacers. 14 Simulated assembly of tetranucleosomes by random placement along the substrates revealed that the interaction of the

nucleosomes promotes nucleosome array compaction.<sup>13</sup> We developed, in this paper, a theoretical model capable of accounting for the role of the DNA sequence and internucleosomal interactions in forming nucleosome structures. These findings suggest that in the chromatin assembly, the affinity of the nucleosomes to the DNA sequence and the strengths of the internucleosomal interactions are the two major factors defining the compactness of the chromatin.

Two types of nucleosomes exist. Canonical nucleosomes  $(H3_{\rm nuc})$  are found throughout the chromosome and consist of two of each histone (H2A, H2B, H3, and H4). The H2A and H2B form dimers and interact with the entry—exit site opposite the H3/H4 tetramer arranged at the dyad. The H3<sub>nuc</sub> wrap ~147 bp of DNA corresponding to ~1.7 turns around the octameric histone core. A unique area of the chromosome is the centromere, which is responsible for holding together the sister chromatid and then must be pulled apart during replication. In the centromere nucleosomes, a variant of H3 histone is replaced with its variant, CENP-A, in the octameric core. CENP-A nucleosomes (CENP-A<sub>nuc</sub>) typically wrap 121 bp. Both types of nucleosomes are dynamic, and in our AFM experiments, we found that CENP-A<sub>nuc</sub> are capable of spontaneous unwrapping, which is the

Received: December 24, 2023 Revised: June 21, 2024 Accepted: June 21, 2024



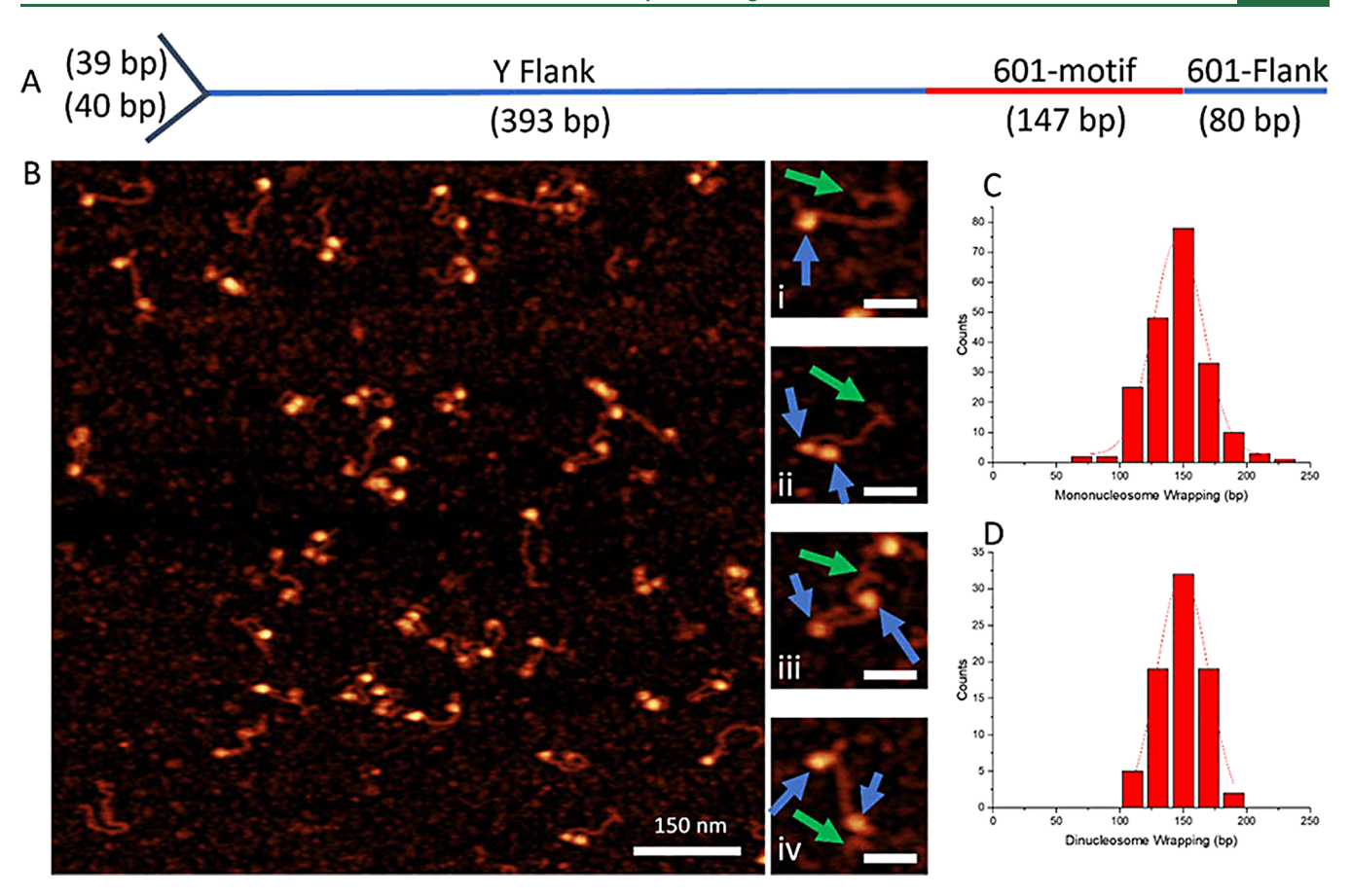


Figure 1. AFM imaging of H3 nucleosomes. (A) DNA construct containing a three-way junction at one terminal end as a fiducial marker, and the 601 motif is shown in red. (B) AFM image 1000 nm  $\times$  1000 nm. Selected zoomed images of monoH3<sub>nuc</sub>(i) and diH3<sub>nuc</sub> (ii, iii, and iv) subsets are shown to the right of the main AFM image. Nucleosomes and 3WJ are indicated with blue and green arrows, respectively. (C, D) Histograms for wrapping efficiencies of mononucleosomes (C) and dinucleosomes (D).

major dynamics pathway.  $^{9,28-30}$  Unwrapped CENP-A nucleosomes can undergo long-range translocation by traveling over  $\sim\!200\,$  bp; this process is also reversible.  $^{28,29}$  Additionally, CENP-A stabilizes nucleosome core particles against complete dissociation even when not fully wrapped with DNA.  $^{28,29}$ 

Here, we compare the nanoscale features of both types of nucleosomes assembled on identical DNA templates. Using the DNA template with segments with different nucleosome affinities capable of forming two nucleosomes, we compared the interactions and dynamics properties of both types of nucleosomes assembled on the same DNA templates. Internucleosomal interaction was estimated by measuring the internucleosomal distance, revealing the elevated interactions between canonical nucleosomes compared with the CENP-A ones. Time-lapse, high-speed AFM (HS-AFM) was applied to characterize the nucleosome's unraveling dynamics, allowing us to reveal similarities and differences between canonical H3 and CENP-A nucleosomes.

### EXPERIMENTAL METHODS

Y-DNA Construct. Our DNA preparation is done in the same way as our lab has done previously using PCR with a pUC57 plasmid vector from BioBasic (Markham, ON, CA). 10,31–33 The 3WJ terminal DNA design was completed by introducing the SapI cut site in the primer (5'-TTAGCGGAAGAGCGCTTGTCTGTAAGCGGATGCCG-3'), with the cut site for SapI being bolded. The SapI cut site allows for modular insertion of the restriction enzyme into any DNA construct. Once SapI cuts the DNA, construct a 3WJ ligated

from three single-stranded DNAs, with the appropriate sticky end ligated to the original DNA. The full-length DNA containing the 3WJ end can be seen in Figure 1. There is a 601 motif that is 80 bp from the non-3WJ end. The rest of the DNA is made of a random sequence with no nucleosome binding specificity.

Nucleosome Assembly H3 and CENP-A. The assemblies of both H3<sub>nuc</sub> and CENP-A<sub>nuc</sub> are completed through 24-h dialysis, starting at 2 M NaCl and ending at 2.5 mM NaCl, the same as we have published previously. <sup>28,30,31</sup> This process occurs at 4C and utilizes a peristaltic pump that continuously pumps the low salt buffer into the reaction beaker at the same rate that it pumps the high salt buffer out. The H3<sub>nuc</sub> is purchased from the Histone Source (Fort Collins, CO) and is already in an octameric form. It requires mixing the nucleosomes and DNA and a predialysis to remove the glycerol from the stock. The CENP-A<sub>nuc</sub> histones are purchased from EpiCypher (Durham, NC) and come in two stocks, one containing the H2A/H2B dimers and one containing the CENP-A/H4 tetramer. They require the extra step of mixing the two histone stocks in equimolar concentrations to obtain an octameric core with two dimers and a single tetramer.

Static AFM Sample Preparation and Imaging. The static AFM samples are prepared after the assembly of the nucleosomes and are deposited on 1-(3-aminopropyl) silatrane (APS) mica, thereby functionalizing the surface of the mica. The stock solutions of H3<sub>nuc</sub> and CENP-A<sub>nuc</sub> are stored at 300 nM at 4C. In preparation for the stock solution for imaging, a small aliquot is taken and diluted to 2 nM using imaging buffer (4 mM MgCl<sub>2</sub> and 10 mM HEPES) and deposited on the APS mica. The mica containing the sample is incubated for 2 min, washed gently with DI water, and dried with a slow argon flow. The sample is placed in a vacuum and allowed to dry overnight under vacuum. The dried samples are then imaged on a

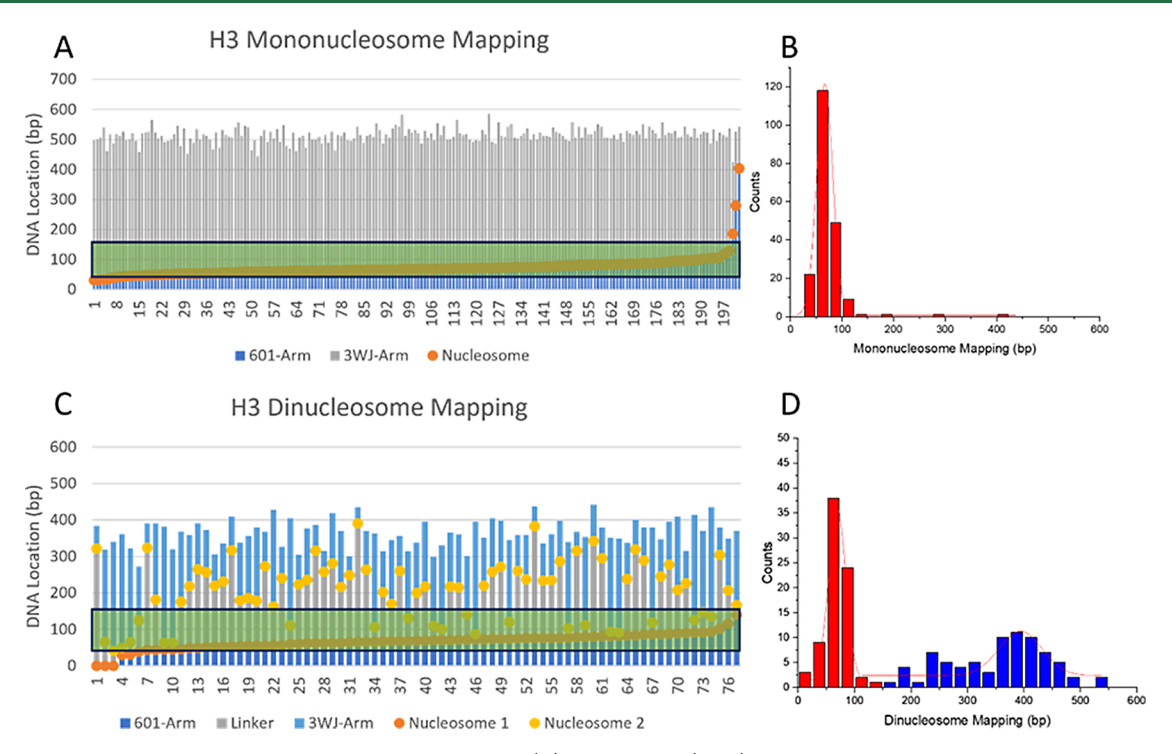


Figure 2. AFM mapping of  $H3_{nuc}$ . The static AFM of mono $H3_{nuc}$  (A) and di $H3_{nuc}$  (A, C) mapping location binding on the DNA construct. The orange and yellow dots are nucleosome binding locations. The *Y*-axis is the DNA location, where 0 indicates the 601 terminal end, and the 601 motif starts 80 bp from 0. The green area represents the 601 area on the DNA. (B, D) Histograms for mapping data for mononucleosomes (B) and dinucleosomes (D). Different colors in D correspond to the nucleosome position on the 601 motif (red) and the rest of the DNA template (blue).

MultiMode AFM/NanoScope IIId utilizing TESPA probes (Bruker Nano Inc., Camarilla, Ca). The static images were captured at  $3 \times 3$   $\mu$ m in size with 1536 pixels/line.

High-Speed Atomic Force Microscopy Imaging in Liquid. High-speed AFM imaging was performed as described in our previous literature.  $^{28,30,34}$  Briefly, a thin piece of mica was punched into 1.5 mm diameter circular pieces and then glued onto the sample stage of the HS-AFM instrument (RIBM, Tsukuba, Japan). 2.5  $\mu$ L portion of 500  $\mu$ M APS solution was deposited onto the mica and incubated for 30 min in a wet chamber to functionalize the mica surface. The mica surface was then rinsed with 20  $\mu$ L of deionized water. Then, 2.5  $\mu$ L of the DNA or nucleosome sample was deposited onto the APS functionalized mica surface and incubated for 2 min. The sample was then rinsed with buffer and put into a fluid cell containing the imaging buffer described above. HS-AFM carried out imaging using electron beam deposition (EBD) tips. The typical scan size was 400 × 400 nm with an 800 ms/frame scan rate.

Data Analysis. We utilize the same methods as previously published by our lab. 28,31 The static images captured are analyzed using FemtoScan (Advance Technologies Center, Moscow, Russia), where we can measure the contour lengths of the DNA. The contour length measurements begin at the end of the 3WJ and are measured to the middle of the nucleosome. The second arm measurement starts at the center of the nucleosome and is measured to the 601 terminal end. Five nm is subtracted from both arm lengths due to the contribution of the DNA to the wrapping around the nucleosome. A conversion factor is calculated from naked DNA to calculate the bp of the measurements. In the static images, measuring the contour lengths of all of the free DNA and dividing by the known DNA length (659) will provide a number around 0.35, which we use to convert nm measurements to bp. The linker length between two nucleosomes is calculated by measuring the DNA length between the center of two nucleosomes and subtracting 10 nm of DNA to account for the contribution of both nucleosomes.

In HS-AFM, the contour length is calculated by measuring the DNA length after the nucleosome has evacuated the DNA, and the full-length DNA is accessible for measurement. The averages of the

contour lengths are used to calculate the conversion factor. The histograms were created by using Origin. Microsoft Excel was used for creating scatter plots and bar graphs.

## RESULTS

**DNA Substrate.** We designed a DNA template capable of assembling two nucleosomes containing the nucleosome-specific 601 motif and non-nucleosome-specific random sequences to accomplish the goal. Schematically, the construct is shown in Figure 1A. At the end of the DNA, opposite to the location of the 601 motif, we placed a three-way junction DNA segment forming a Y-shape, which served as the marker for mapping the nucleosomes on the DNA. The nucleosomes were assembled as described in the Methods section using a 2:1 molar ratio of the nucleosome core and DNA. The samples with CENP-A<sub>nuc</sub> and canonical H3<sub>nuc</sub> were assembled in parallel and prepared for AFM imaging as described earlier. <sup>30,31</sup>

Positioning for Canonical H3 Nucleosomes. Figure 1B shows typical topographic AFM images for the array with a canonical H3<sub>nuc</sub> sample. Nucleosomes appear as bright globular features, and mononucleosome samples are seen along with dinucleosomes. Selected images for mono and dinucleosomes are shown to the right of the scan. The frame (i) shows a mononucleosome AFM image in which the nucleosome is indicated with a blue arrow, whereas the green arrow points to the Y-end of the DNA. Three other frames (ii)—(iv) illustrate dinucleosome samples with different distances between the nucleosomes indicated with blue arrows. The nucleosomes were found in close locations (frame (ii)) or far from each other (frames (iii) and (iv)). The AFM images were analyzed to characterize the arrays.

First, the length of DNA wrapped around the nucleosome was measured to determine the length of DNA wrapped

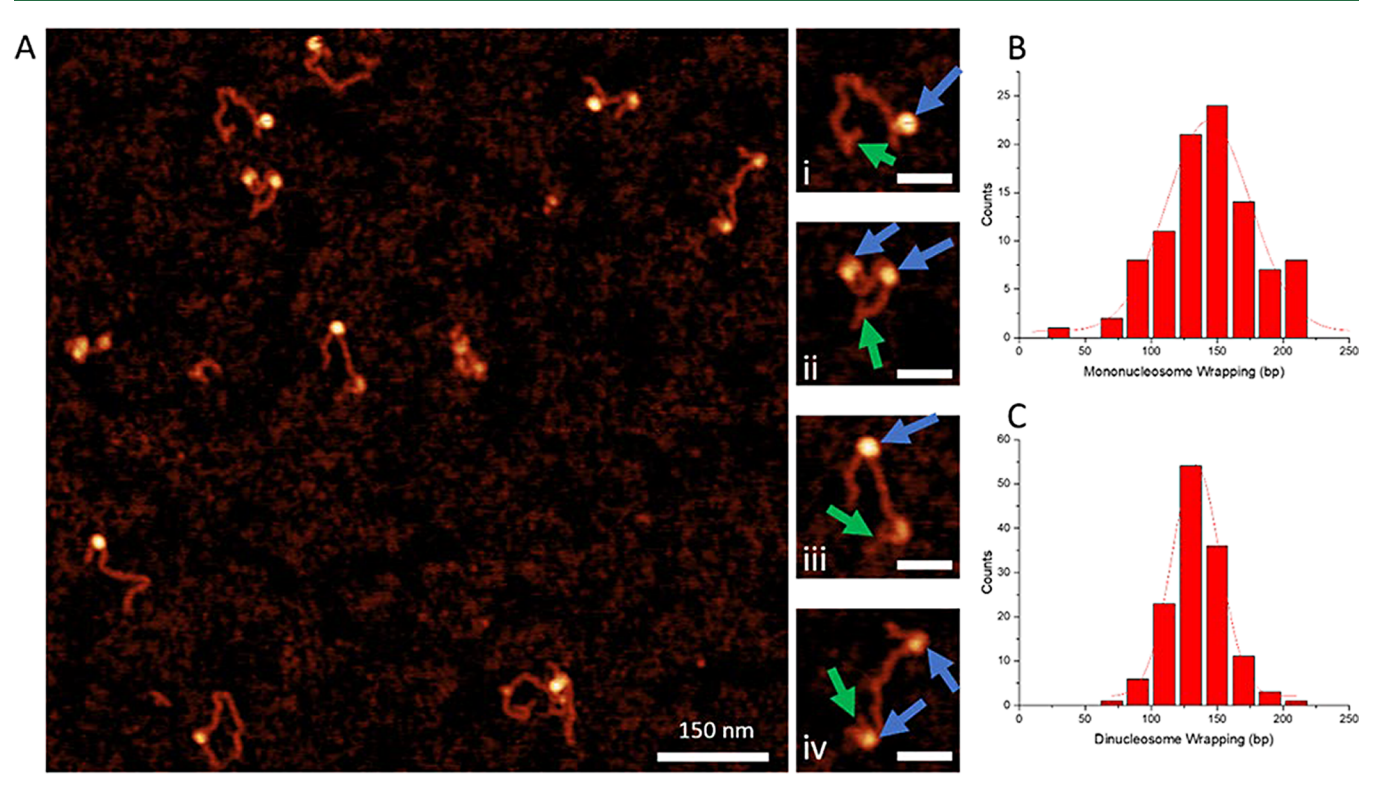


Figure 3. AFM imaging of CENP-A nucleosomes. (A) AFM image of 1000 nm  $\times$  1000 nm. Selected zoomed images of monoCENP-A<sub>nuc</sub> (i) and (iii) and diCENP-A<sub>nuc</sub> (ii) and (iv) subsets are shown to the right of the main AFM image. Nucleosomes and 3WJ are indicated with blue and green arrows, respectively. (B, C) Histograms for wrapping efficiencies of mononucleosomes (B) and dinucleosomes (C).

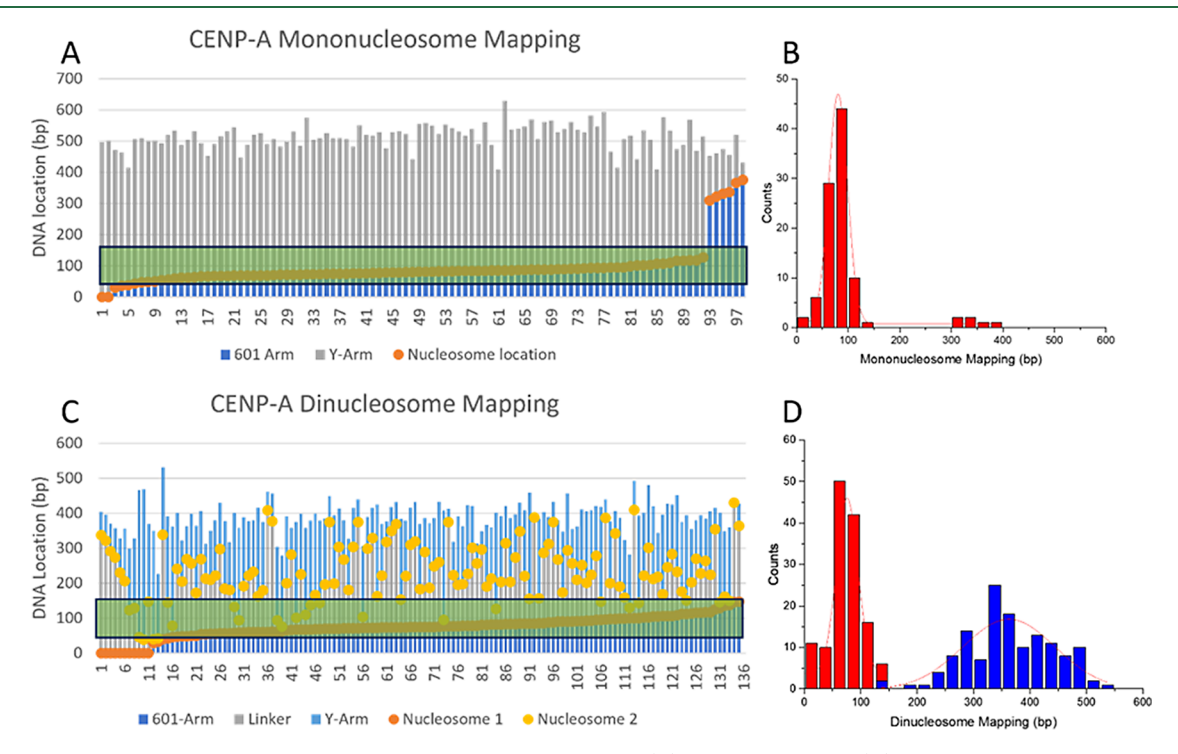


Figure 4. AFM mapping of CENP- $A_{nuc}$ . The static AFM of monoCENP- $A_{nuc}$  (A) and diCENP- $A_{nuc}$  (C) AFM mapping location binding on the DNA construct. The orange and yellow dots are nucleosome binding locations. The Y-axis is the DNA location, where 0 indicates the 601 terminal end, and the 601 motif starts 80 bp from 0. The green area represents the 601 area on the DNA. (B, D) depict histograms for mapping data for mononucleosomes (B) and dinucleosomes (D). Different colors in D correspond to nucleosome position on the 601 motif (red) and the rest of the DNA template (blue).

around the core and the wrapping efficiency. It was done by subtracting the total contour lengths of DNA segments

attached to the nucleosome core from the total length of the free DNA. The mono- and dinucleosome sample data are

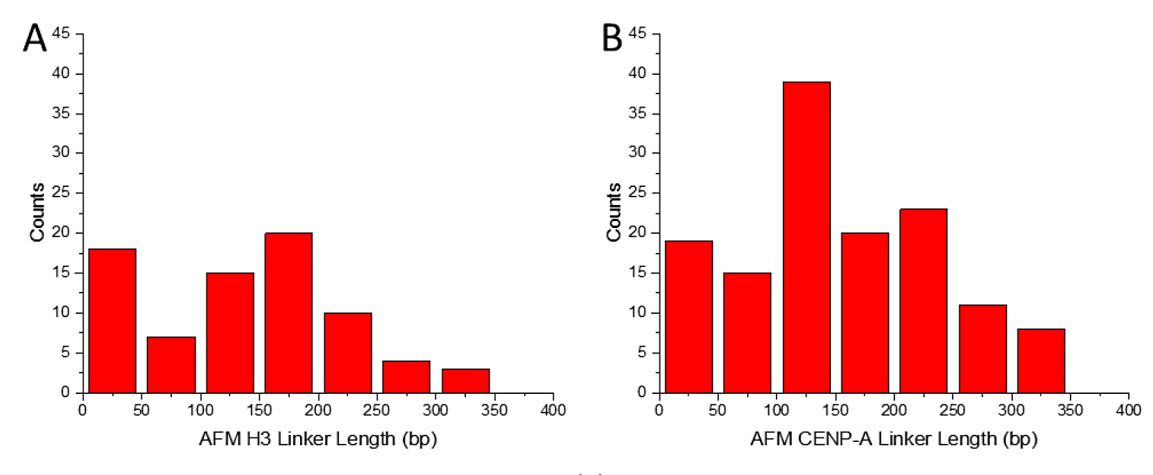


Figure 5. Dinucleosome linker length results. The  $H3_{nuc}$  linker length (A) shows a preferential linker length of less than 50 bp and a Gaussian distribution of around 170 bp. The CENP- $A_{nuc}$  linker length (B) demonstrated a lower yield of linker lengths of less than 50 bp and the largest population of around 125 bp.

shown in Figure 1C,D, respectively. These data demonstrate that the monoH3<sub>nuc</sub> wrap 145  $\pm$  23 bp and the diH3<sub>nuc</sub> wrap 149  $\pm$  24 bp, which are in the expected 147 bp value range. <sup>35,36</sup>

Next, we mapped the positions of the nucleosomes for both types of samples. The data visualizing the positions of the center of the nucleosomes for the mononucleosome samples are shown in Figure 2A. The green highlighted area indicates the 601 location on the DNA construct. The zero position on the *Y*-axis corresponds to the DNA end opposite the 3WJ. The positions of the nucleosome center are marked with orange dots. The primary binding locations of nucleosomes are to the 601 sequence (orange dots)—only three nucleosomes out of 202 (99%) bind to the locations outside the 601 region. The histogram of the nucleosome position in Figure 2B produces a narrow distribution.

A similar mapping analysis was performed for the dinucleosome samples, and the results are assembled in Figure 2C. Nucleosomes bound to the 601 region are depicted as orange dots, and the position of the second nucleosome is shown as yellow dots. The positions of the yellow dots are not specific, so these are scattered over the rest of the DNA template. The histograms for the nucleosome positions assembled as histograms are shown in Figure 2D. A narrow peak (red) corresponds to the nucleosome assembled at sequence 601, and the positions of the second nucleosome shown in blue are not well-defined, producing a broad peak.

**Positioning for CENP-A Nucleosomes.** Typical AFM images for the CENP- $A_{nuc}$  samples are shown in Figure 3A with selected zoomed images of the subset's mono- and dinucleosome species. In frame (i), a mononucleosome (blue arrow) can be seen bound to the 601 site, far from the 3WJ (green arrow) at the opposite end of the DNA. In frame (ii), two nucleosomes are relatively close to one another. In frame (iii), there is one stable nucleosome fully wrapped near the 601 site, and near the 3WJ, there is an unwrapped nucleosome. In frame (iv), two partially unwrapped nucleosomes are bound to the DNA.

The measurements of the DNA wrapping efficiency for CENP-A $_{\rm nuc}$  were done in the same way as that for the H3 $_{\rm nuc}$  samples. The monoCENP-A $_{\rm nuc}$  samples had a DNA wrapping efficiency of 137  $\pm$  43 bp; the standard deviation for the monoCENP-A $_{\rm nuc}$  wrapping is much larger than that for the H3 $_{\rm nuc}$  counterpart. The dinucleosome assemblies of the

CENP- $A_{nuc}$  DNA wrapping efficiency were 130  $\pm$  20 bp. Histograms for the bp wrapping of mononucleosomes and dinucleosomes can be seen in Figure 3B,C, respectively.

The mapping of CENP- $A_{nuc}$  was completed on the same DNA construct as the  $H3_{nuc}$ . The monoCENP- $A_{nuc}$  mapping results can be seen in Figure 4A.

The mapping results for the dinucleosome CENP-A<sub>nuc</sub> sample (diH3<sub>nuc</sub>) are shown in Figure 4C. The orange dots are the nucleosomes bound closer to the non-3WI end, which results in 93% of the nucleosomes binding to the 601 sequence. The yellow dots represent the nucleosomes binding closer to the 3WJ end, which comprises nonspecific DNA; therefore, the nucleosomes have random binding locations. Interestingly, there is an elevated affinity for the CENP-A<sub>nuc</sub> assembly at the end of the DNA template. The green highlighted area shows the location of the 601 sequence on the DNA construct. The orange dots represent the center of the nucleosome binding location. The blue arm represents the DNA from the center of the nucleosome to the non-3WJ terminal end, and the gray bars represent the DNA from the center of the nucleosome to the 3WJ terminal end. The high affinity of the nucleosomes to the 601 motif is seen in these nucleosomes, although there is a decrease to 92% binding to the specific sequence as compared with 99% for H3<sub>nuc</sub>. A histogram representation of the CENP-A<sub>nuc</sub> binding location can be seen in Figure 4B, showing specific binding to the 601 region.

Internucleosomal Interactions for H3 and CENP-A **Nucleosomes.** Nucleosomes in the AFM images (e.g., plate ii in Figure 1B) are located close to each other, pointing to the interaction between the nucleosomes. Such events can be identified in dinucleosome maps (Figure 5) by the colocalization of two nucleosomes. We used the values for the nucleosome locations' centers to measure the linker length's internucleosomal distance to characterize the ratio of such close contacts. 10 The results of such measurements for canonical H3 dinucleosomes are shown as histograms in Figure 5A. The first bar in the histogram corresponds to the close location of the nucleosome, which, according to our publication, 10 points to the formation of close internucleosomal contacts. The yield of nucleosomes with a linker length of less than 50 bp was 23%. A similar analysis was done for the CENP-A dinucleosomes, and the histogram is shown in Figure 5B. Although the bar corresponding to the distance below 50

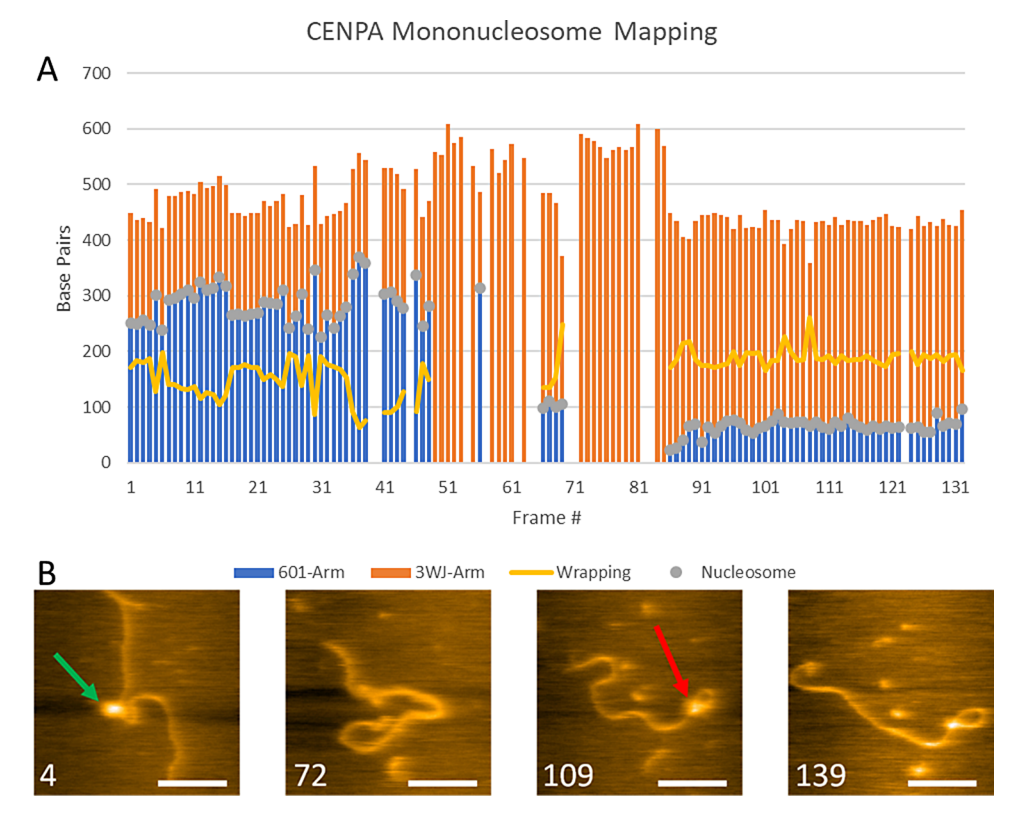


Figure 6. (A,B) High-speed AFM video analysis. Movie S1 analyzed, showing the mapping (bar graph) and snap shots of particular frames. The gray dots in the bar graph indicate the nucleosome bound to the DNA. The yellow line shows the bp of DNA wrapping around the CENP-A nucleosome. The number in white at the bottom left of the snapshots indicates the frame from which the image is taken. The scale bar is 50 nm.

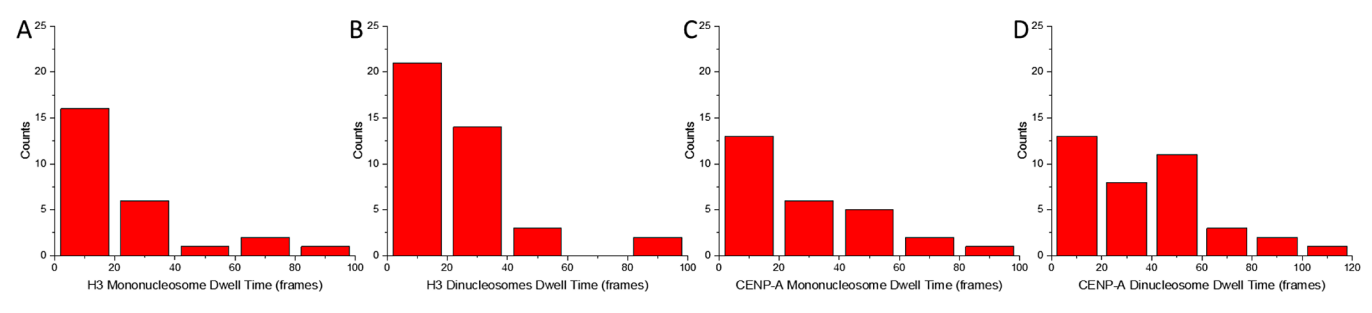


Figure 7. Nucleosome dwell times on HS-AFM. The monoH3<sub>nuc</sub> results (A) showed most nucleosomes lasting 20 frames or less. The diH3<sub>nuc</sub> results (B) showed a shift to the right, indicating that the dinucleosomes have a dwell time longer than that of the mononucleosomes. The monoCENP-A<sub>nuc</sub> results (C) showed that most nucleosomes lasted less than 20 frames. The diCENP-A<sub>nuc</sub> results (D) showed a shift to the right, indicating that the dinucleosomes have a longer dwell time than the mononucleosomes.

nm is detectable, its height is twice as low as that for  $H3_{nuc}$  (Figure 5A), pointing to the weaker internucleosomal interactions for CENP- $A_{nuc}$  compared with  $H3_{nuc}$  ones. The error of measurements was calculated by measuring 35 particles approximately 20 times each and calculating the standard deviation. With approximately 700 measurements, the standard deviation was  $\pm 1.3$  nm ( $\pm 2.8$  bp).

Time-lapse AFM to Probe Nucleosome Dynamics. Nucleosomes are dynamic complexes capable of spontaneous dissociation, which were directly characterized by single-molecule approaches. AFM is attractive among these methods because it can directly visualize the spontaneous unraveling of nucleosomes using the time-lapse AFM approach. In this approach, the sample is placed on the substrate, and continuous scanning over the same area allows one to observe the dynamics of various systems, including nucleosomes. We applied high-speed AFM capable of data

acquisition in the millisecond time scale<sup>34,41</sup> to compare the dynamics of two types of nucleosomes characterized above.

Multiple frames are acquired, and a set of time-lapse images over the same area is shown in Figure 6 to illustrate a spontaneous unraveling of the nucleosome—the complete set of data sets with 211 frames assembled as Movie S1 is shown in the supplement. There were approximately 100 videos analyzed in total for H3<sub>nuc</sub> and CENP-A<sub>nuc</sub>, which resulted in 4113 total frames being analyzed. In frame 4, the nucleosome is fully wrapped in a random location (green arrow) in the middle of the DNA. In frame 72, the nucleosome has disassociated completely from the DNA. In frame 109, a nucleosome rewraps DNA, spontaneously assembling a nucleosome. This assembly remains stably wrapped up to frame 139.

**Dwell Time for Nucleosomes Unraveling.** One of the parameters that we analyzed was the dwell time of the

nucleosome, defined by the time required for the complete unraveling of the nucleosome. First, we compared the dwell times of mono and dinucleosomes, and the results for H3<sub>nuc</sub> can be seen in Figure 7A,B, respectively. For mono H3<sub>nuc</sub>, we found that 62% (16/26) of the videos analyzed lasted 20 frames or less, videos that lasted 20 to 40 frames were 23% (6/ 26), and videos lasting between 40 and 60 frames were 4% (1/ 26). These lengths of the videos are increased when looking at the dinucleosome dwell times with videos lasting less than 20 frames, between 20 and 40 frames, and between 40 and 60 frames being 53% (21/40), 35% (14/40), and 8% (3/40), respectively. These results show a ratio of 16:6:1, demonstrating that short videos are more than 2.5 times more common than 20 to 40 frame videos. This ratio is decreased when looking at the dwell times of the  $diH3_{nuc}$  with a ratio of 21:14:3; the dwell time of less than 20 frames was 1.5 times more likely to occur. Similarly, the dwell time was analyzed for CENP-A<sub>nuc</sub> samples, and the data are summarized in Figure 7C,D. We found that the dwell time for monoCENP-A<sub>nuc</sub> was 48% (13/27), 22% (6/27), and 19% (5/27) for videos less than 20 frames, between 20 and 40, and between 40 and 60 frames, respectively. Next, we analyzed the dwell time for diCENP-A<sub>nuc</sub>, which was 34% (13/38), 21% (8/38), and 29% (11/38) videos with less than 20 frames, between 20 and 40, and between 40 and 60 frames, respectively. A similar analysis was completed on the frame analysis in supplementary Figure S1, where a direct visual comparison of lifetimes of mono- and dinucleosomes (H3 and CENP-A) demonstrates that dinucleosomes almost always had a longer dwell time (bar height). This figure demonstrates that gray bars (mononucleosomes) are lower than red ones (dinucleosomes). Taller bar heights for each type of nucleosome support the elevated longevity of CENP-A $_{\rm nuc}$  compared with H3 $_{\rm nuc}$ .

Dynamics of Nucleosomes Core During Unraveling. This large set of data revealed that unraveling is a nongradual process. It is illustrated in Figure 8. One set of images is shown in Figure 8A (Movie S2). In Figure 8A, it can be seen that there is an H3<sub>nuc</sub>(green arrow) that is wrapped at the 601 location (frame A1). In the following frames (A2 and A20), the histone (blue arrow) has vacated the octameric core, but the partial core remains to wrap the DNA. In frame A36, the DNA unwraps the partial core, resulting in a wrapping of  $\sim 100$ bp, and the free histone remains near. In the last frame, A66, the only histone remaining appears to be the tetramer. These predictions on the dimer being the first to leave the octameric core are based on the size of the histone leaving, the location, and the assembly process of nucleosomes, showing that dimers are the last ones to leave; it would make sense that they would be the first histones to leave.

 ${
m H3}_{
m nuc}$  (green arrow), in Figure 8B, starts fully wrapped at the 601 location (frame B1). In frames B4 and B7, it can be seen that a histone (blue arrow) left the core particle and now drifts nearby. During this process, unwrapping of the DNA took the  $\sim$ 150 bp wrapping down to  $\sim$ 100 bp in frame B4. This unwrapping continues, and by frame B11, the core particle is no longer wrapping any DNA. We assume that the octameric core splits into its three components:  ${
m H2A/H2B}$  dimers (blue arrows) and the  ${
m H3/H4}$  tetramer (yellow arrows).

Next, we looked at the unwrapping pathways of CENP- $A_{\rm nuc}$  on the same DNA construct. Figure 9A (complete set of frames in Movie S6), frame A1 shows a fully wrapped CENP- $A_{\rm nuc}$  (green arrow) bound to the 601 site. The nucleosome remains stably wrapped in frames A4 to A18. In frame A20, the

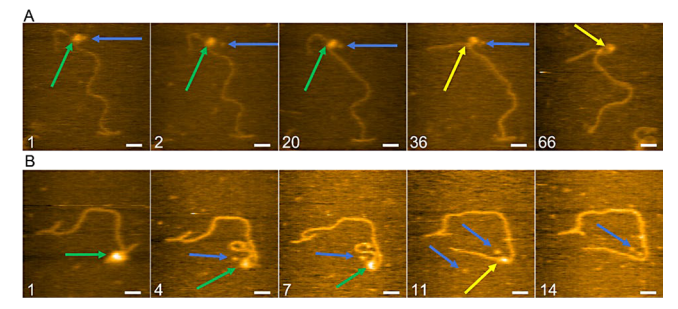
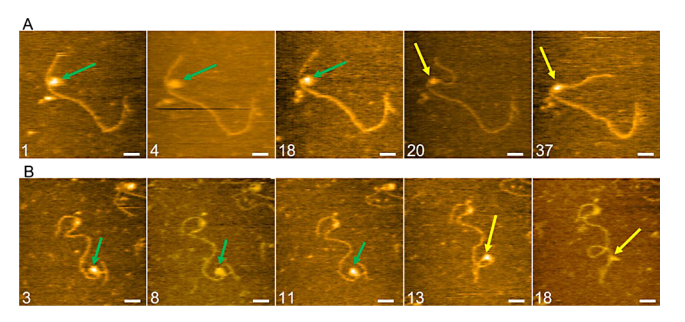


Figure 8. HS-AFM analysis of H3<sub>nuc</sub>unwrapping. HS-AFM videos analyzed, showing the protein unwrapping pathway of H3<sub>nuc</sub>(green arrows) with histones (blue arrows) leaving the nucleosome core particle. Once the DNA unwraps the nonoctameric core, they are indicated with yellow arrows—the frames in A come from Movie S2. In frame A1, the nucleosome is bound to the 601 location, and the histone can be seen bulging out, indicated with the blue arrows. This histone moves in frames A2 and A20, while the DNA and nucleosomes remain in the same location. In frame A36, the DNA unravels the nucleosome; by frame A66, only the tetramer can be seen still bound to the DNA. The frames in B come from the video of Movie S3. In frame B1, the green arrow indicates a fully wrapped nucleosome bound to the 601 location. In frames B4 and B7, the histone (green arrow) can be seen to have left the nucleosome core particle, leaving a partial core. By frame B11, the DNA has unwrapped the partial core, and the tetramer remains bound. By frame B14, all histones have evacuated the DNA. The scale bar is 25 nm.



**Figure 9.** (A,B) HS-AFM analysis of CENP- $A_{nuc}$  unwrapping. AFM videos were analyzed, showing the DNA unwrapping pathway of CENP- $A_{nuc}$  (green arrows). The scale bar represents 25 nm.

nucleosome (yellow arrow) spontaneously unwraps, resulting in a decreased wrapping of  $\sim\!110$  bp. The CENP- $A_{\rm nuc}$  remains wrapped  $\sim\!110$  bp through the next frame shown, A37. The example in Figure 9B (Movie S7) shows a CENP- $A_{\rm nuc}$  bound near the 3WJ (frame B3). The CENP- $A_{\rm nuc}$  (green arrow) remains stably wrapped at this location through frames B8 to B11. In frame B13, the nucleosome (yellow arrow) undergoes unwrapping, resulting in a wrapping of  $\sim\!100$  bp. By frame B18, the nucleosome no longer wraps any DNA. Notably, no octamer dissociation was observed during the entire unraveling process, both on and off the 601 sequence.

The nucleosome core stability of H3<sub>nuc</sub> was found to be weaker through our analysis of the HS-AFM videos. We found that out of 69 total movies of H3<sub>nuc</sub> analyzed, 53 (77%) of them resulted in the nucleosome core losing histones during the unwrapping, as indicated in Figure 5A,B; the blue arrows are pointing to the histones leaving the nucleosome core. In contrast, CENP-A<sub>nuc</sub> had 63 nucleosomes analyzed, and only 6 (10%) had histones leave the core during the unwrapping event, indicating that the DNA was able to unwrap the nucleosome core without the octameric core falling apart.

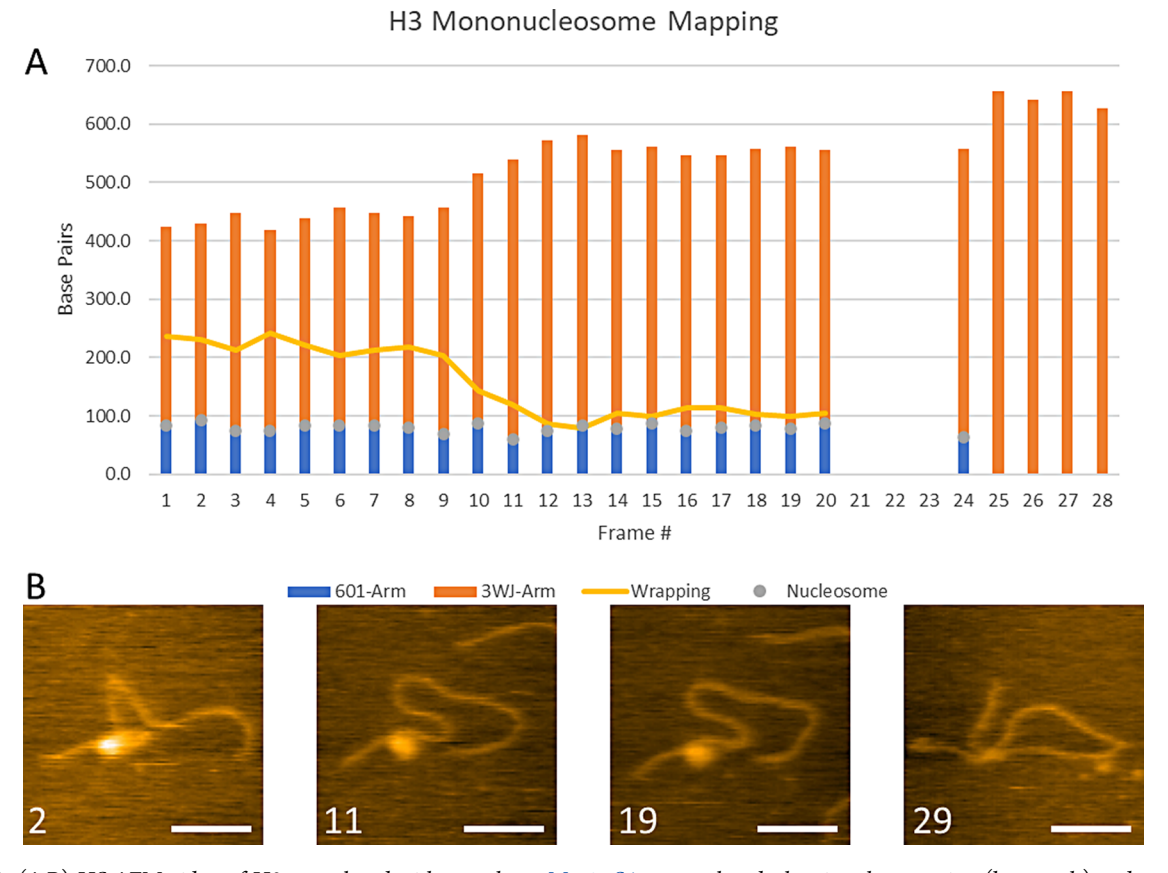


Figure 10. (A,B) HS-AFM video of  $H3_{nuc}$  analyzed with snapshots. Movie S4 was analyzed, showing the mapping (bar graph) and snapshots of particular frames. The orange bars represent the DNA from the 3WJ end to the center of the nucleosome (gray dot). The blue bar represents the 601 DNA from the 601 end to the center of the nucleosome. The yellow line shows the bp of DNA wrapping around the  $H3_{nuc}$ . The number in white in the bottom left of the snapshots indicates the frame of the image.

These results lead us to believe that the CENP- $A_{\rm nuc}$  core particle is significantly more stable than  $H3_{\rm nuc}$ , which likely plays a role in its necessity of having a strong interaction to withstand the kinetochore pulling the sister chromatid apart. This overall higher stability of CENP- $A_{\rm nuc}$  is also supported by the longer dwell times found with CENP- $A_{\rm nuc}$  compared to the  $H3_{\rm nuc}$ , as seen in Figure 7.

**Nucleosome Stepwise Unraveling.** AFM images shown above point to the stepwise process of the nucleosome unraveling. To characterize this phenomenon, we measured the lengths of the DNA arms for each frame and plotted these measurements as a set of bars with different colors. These data are shown in Figure 10A, and a few snapshots are displayed in Figure 10B.

The complete set of frames is assembled into Movie S4. The blue bars represent the distance from the 601 end of the DNA to the center of the nucleosome (gray dot). The orange bar represents the distance from the center of the nucleosome to the end of the 3WJ. The yellow line shows the DNA wrapping values calculated from the length measurements of the arms. In this set of images in frame (2), the nucleosome can be seen to be overwrapped. These data show that there was a partial unwrapping event that started in frame (11) and proceeded to frame (13), where the nucleosome went from a state of overwrapped (~210 bp) and, throughout three frames, decreased to an under-wrapped state (~100 bp), where it remained bound for another seven frames. The last frame 29 shows the nucleosome wholly disassociated from the DNA.

A similar event is shown in Supplementary Figure S1 and Movie S5. It was demonstrated that the initial overwrapped state ( $\sim$ 200 bp) in frame 10 dropped quickly to an underwrapped state ( $\sim$ 100 bp), where it remained for another six frames.

Both videos demonstrated an intermediate step in H3<sub>nuc</sub> disassembly, a state in which the nucleosome is considerably stable. There was a variation in the time at which these unwrapping events took place. In Movie S4, the unwrapping took place over 3 frames (2.4 s), whereas in Movie S5, the unwrapping took place over 1 frame (0.8 s). The difference in the time to unwrap indicates that there is still something not completely understood in this process.

A similar analysis was done on CENP- $A_{\rm nuc}$ . The data are shown in Figure 11, where the results of measurements are shown (Figure 11A), and snapshots are displayed below (Figure 11B). The complete set of frames is assembled into Movie S8. In the snapshots shown, frames (4) to (36) show a fully wrapped nucleosome, and frame (43) shows an increase in DNA length and a decrease in bp wrapping around the nucleosome. Finally, frame (79) shows histones bound to the DNA without wrapping. In Figure 11A, the CENP- $A_{\rm nuc}$  was stably wrapped ( $\sim$ 130 bp) for 41 frames, at which point, it went to an unwrapped state ( $\sim$ 90 bp). The unwrapping process took only a single frame (0.8 s).

Another video with the same analysis was done to confirm the stepwise disassembly process observed in the previous video, as seen in supplementary Figure S2. This video demonstrates an event similar to that in Figure 10. The

# CENP-A Mononucleosome Mapping

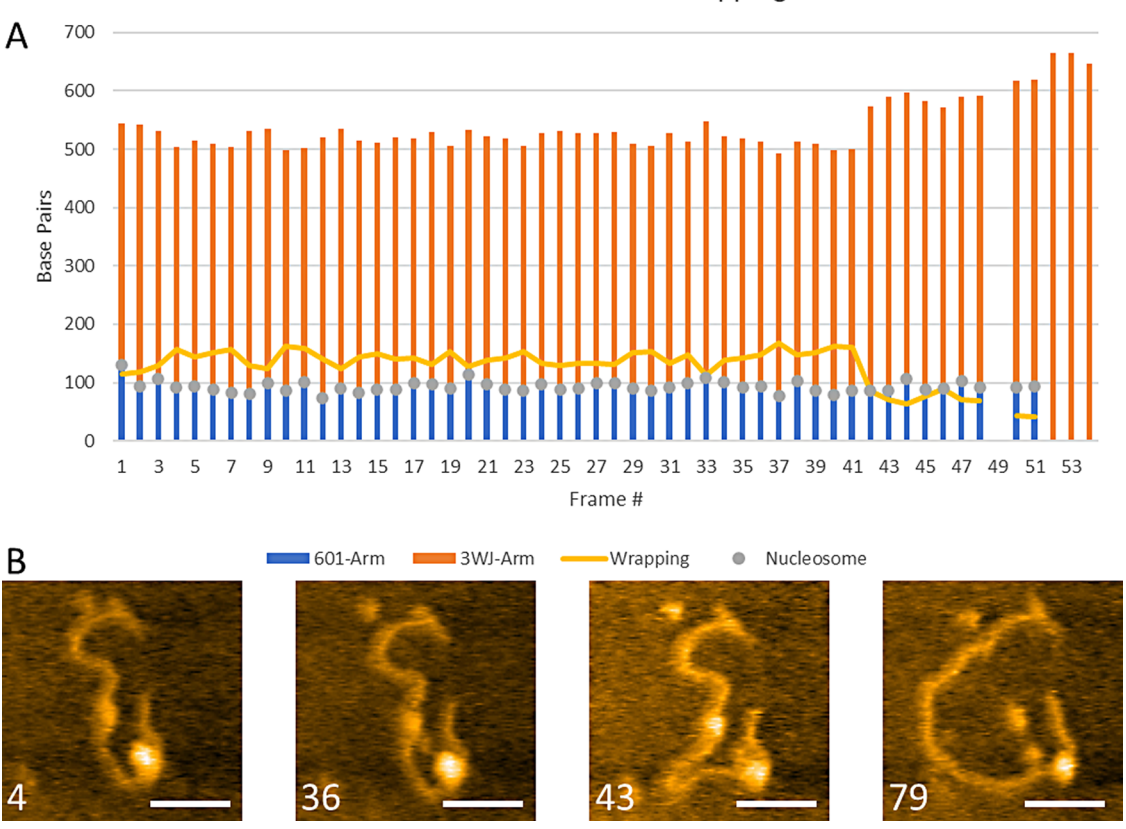


**Figure 11.** (A,B) HS-AFM video of CENP- $A_{nuc}$  analyzed with snapshots. Movie S8 was analyzed, showing the mapping (bar graph) and snapshots of particular frames. The gray dots in the bar graph indicate the nucleosome bound to the DNA. The orange bars represent the DNA from the 3WJ end to the center of the nucleosome (gray dot). The blue bar represents the 601 DNA from the 601 end to the center of the nucleosome. The yellow line shows the bp of DNA wrapping around the CENP- $A_{nuc}$ . The number in white in the bottom left of the snapshots indicates the frame of the image.

ī

nucleosome began in an overwrapped state (~200 bp), remaining for 33 frames. The nucleosome was unwrapped from frames 33 to 35 to ~100 bp, staying for another 12 frames before completely disassociating. It is also important to note that in Supplementary Figure S2, it can be seen that the nucleosome only unwraps from a single side, the 601 arm side unwraps, while the 3WJ arm remains a consistent length.

Asymmetric Unraveling of Nucleosomes. A closer analysis of the H3<sub>nuc</sub> (Figures 10 and S3) and CENP-A<sub>nuc</sub> (Figures 11 and S2) movies revealed that the unwrapping process is asymmetric; therefore, one arm increases the size without changing another arm in length. In Figure 10A, the H3<sub>nuc</sub> short 601 arm (blue) remains constant throughout the video, but the 3WJ arm (orange) increases in length during the unwrapping. Similar asymmetry was observed for the nucleosome initially assembled away from the 601 motif (Figure S2). The 601 arm fluctuated, but the 3WJ arm grew as unwrapping occurred, indicating a single-sided, asymmetrical unwrapping.

The asymmetry in the unwrapping was observed for CENP-A nucleosomes, which is illustrated in Figure 11. The nucleosome is bound to the 601 site, and the short arm (blue) remained constant throughout the video; however, the 3WJ arm (orange) grew in length during the unwrapping. In supplementary Figure S3, the CENP-A<sub>nuc</sub> was assembled near the middle of the DNA template, away from the 601 motif. The nucleosome length of both arms remained relatively consistent until the unwrapping event, which caused the blue

arm to grow in length, with the orange bar remaining constant. Thus, the asymmetric unwrapping events do not indicate a preference for the DNA sequence.

In the analysis of 98 total unwrapping events, asymmetric unwrapping was found in 87% of cases for  $H3_{\rm nuc}$  and 88% of the cases for CENP- $A_{\rm nuc}$ . The symmetric unwrapping was observed in 13 and 12% yields for  $H3_{\rm nuc}$  and CENP- $A_{\rm nuc}$ , respectively.

## DISCUSSION

The dinucleosome approach using end-labeled DNA revealed several different features of CENP-A<sub>nuc</sub> and bulk H3<sub>nuc</sub>. Although both nucleosome types can form tight contacts with no visible space between nucleosomes (Figure 1B, frame ii), CENP-A<sub>nuc</sub> indicated a lower effect than H3<sub>nuc</sub> ones (Figure 5). We have demonstrated that the balance between energies of internucleosomal interaction and the affinity of the nucleosome core to the DNA sequence previously defines the formation of tight contacts between the nucleosomes. 10,13 The balance favors the dinucleosome assembly for nonspecific DNA sequences. We have shown that the number of such contacts increases in nucleosomes assembled with truncated H4 histone, suggesting that histone tails contribute to the tightening of dinucleosomes. 10 Therefore, we hypothesize that the lower yield of dinucleosome complexes for CENP-A<sub>nuc</sub> can be due to the repulsion generated by the CENP-A tail, and we

are currently planning these experiments to test this hypothesis.

The smaller amounts of very close interactions between CENP-A nucleosomes may play a role in centromere formation. There are different theories on the nucleosomal composition of the centromere, with one or a few CENP-A nucleosomes flanked by H3 nucleosomes, or there may be a cluster of CENP-A nucleosomes outward facing on the centromere to interact with the kinetochore. 42–46 Our results show less propensity for CENP-A nucleosomes to bind extremely close to one another; although the difference is small, it may play a role in the CENP-A/H3 nucleosome arrangement in the centromere.

The DNA sequence is the primary factor defining the nucleosome positioning in the chromatin, and the 601 motif is the strongest nucleosome positioning sequence—our AFM data in Figures 1B and 3A visually support it, illustrating the almost exclusive formation of mononucleosomes on the position of the 601 motif. At the same time, there is a difference between these two types of nucleosomes. The yield of H3<sub>nuc</sub> bound to the 601 site in the mononucleosome and dinucleosome samples was 99% (Figure 2B,D). The CENP-A<sub>nuc</sub> were mapped similarly to H3<sub>nuc</sub> and found bound to the 601 site at 92% for mononucleosomes and 93% for the dinucleosomes (Figure 4B,D). These differences in the binding affinity to 601, although marginal ~6%, were consistent in both the mono and dinucleosomes results. Although the DNA sequence and specifically the TA dinucleotides provide such a high affinity of 601 to the formation of nucleosomes, it was shown in 47 that interaction with histones contributes to the nucleosome positioning, and H3-H4 tetramer dominates in the DNA sequence dependency effect. Replacement of the H3 histone with the CENP-A histone can decrease this DNA affinity effect.

A number of novel features of nucleosome dynamics were identified in the time-lapse AFM studies. One is the elevated stability of CENP-A nucleosomes compared with H3 nucleosomes. The stability of nucleosomes was characterized by the dwell time prior to the unwrapping, and according to Figure 7, 38% of monoH3<sub>nuc</sub> lasted longer than 20 frames, whereas 52% of monoCENP-A<sub>nuc</sub> lasted longer than 20 frames, which is a 14% increase in the dwell time. This finding seems counterintuitive as the wrapping efficiency of CENP-A<sub>nuc</sub> is less than H3<sub>nuc</sub>. However, CENP-A nucleosomes are not simply partially unwrapped H3 nucleosomes. Structures of CENP-A and H3 nucleosomes are different, pointing to different contacts between the DNA and histones; therefore, this structural property of these two types of nucleosomes explains their different stabilities. For example, the CENP-A nucleosomes have increased flexibility of the DNA ends, the octameric core is more rigid, and has a different surface charge (positive) at the interface of the L1 of CENP-A and L2 of H4; in contrast, this surface is negatively charged in <sup>27,48</sup> The internucleosomal interaction further increases the nucleosome stability of CENP-A nucleosomes, which can be explained by the different internucleosomal contacts of these two types of nucleosomes. Unwrapping pathways for both types of nucleosomes are different, as well. Most commonly, unwrapping of H3<sub>nuc</sub> occurs through the loss of histones from the nucleosome core, apparently an H2A/H2B dimer. 49-51 According to 18, the remaining dimer sits at the entry-exit site opposite the tetrameric H3/H4 dimer at the nucleosome's dyad. This finding is in line with the recent

publication. <sup>52</sup> Interestingly, their experiments utilized bare mica, a negatively charged surface, whereas our experiments utilized APS functionalized mica, which is a positively charged surface. However, our experimental results aligned well, further validating the experiments. Following the loss of the dimeric histone, the nucleosome unwraps from  $\sim$ 147 bp to a less wrapped assembly with  $\sim$ 100 bp of wrapped DNA. In the H3<sub>nuc</sub>, a hexasome with a single dimeric H2A/H2B can maintain the integrity of a single DNA wrap around the histones.

The increase in dwell times for CENP-A is likely biologically relevant due to the strain that the CENP-A nucleosomes experience during sister chromatid separation, making it necessary for these centromeric nucleosomes to have a stronger interaction with the DNA than what is necessary in the rest of the chromosome.

The unwrapping of the CENP-A nucleosomes is entirely different. According to the data in Figure 9, the CENP-A<sub>nuc</sub> unwrap without the loss of histones. Such an elevated stability of the histone core for CENP-A nucleosomes is in line with our early observations, <sup>28</sup> wherein the long-range translocation of the CENP-A nucleosome core, including its transfer from one DNA molecule to another, was observed in the HS-AFM experiments. Conversely, H3<sub>nuc</sub> had a much higher occurrence of histones vacating the octameric core. In Figure 9A, the CENP-A<sub>nuc</sub> (green arrow) can be seen sitting at the 601 location in frames A1, A4, and A18. In frame B20, the DNA on the short arm can be seen to have lengthened, indicating an unwrapping of the nucleosome (yellow arm now). Of note, no histones left the nucleosome during this unwrapping transition. The under-wrapped nucleosome can be seen stably bound to the DNA in frame A37, still at the 601 location.

We also found that the disassembly process for both  $\rm H3_{nuc}$  and CENP- $\rm A_{nuc}$  is not gradual but stepwise. According to Figures 10 and 11, the unwrapping results in a relatively stable state of the nucleosomes with ~110 bp of wrapped DNA. At this transient state, one entry/exit DNA length remains completely intact, while the other unraveled between 20 and 40 bp. These results give insights into how the nucleosomes may be translocated in a rolling fashion, breaking only the contacts on a single side. The stepwise nucleosome unwrapping is in line with the recent publication, <sup>52</sup> although it was observed for H3 nucleosome only. We show here that stepwise unwrapping is the typical dynamics property of both types of nucleosomes regardless of the differences in the pathways of the unwrapping process.

The asymmetric unwrapping of the nucleosomes is another property observed in both nucleosome types. Asymmetry is the preferential pathway for the unwrapping of nucleosomes, which was observed in 87% of cases for H3<sub>nuc</sub> and 88% of the CENP-A<sub>nuc</sub>. Previously, asymmetry was observed for the initial stage of unwrapping for the breathing of DNA.<sup>53</sup> Other published works discovered that the histone dimers (H2A/ H2B) are the first to leave the octameric core, guided by the asymmetrical unwrapping of the DNA. 51,54 Here, we observed asymmetry in the nucleosome unwrapping over the entire unraveling process. Also, we observed the asymmetry in unwrapping for CENP-A nucleosomes, where the core remains intact, suggesting that core dissociation is not a factor contributing to the asymmetry of nucleosome unwrapping. Qualitatively, asymmetric unwrapping can be explained by the fact that DNA within nucleosomes is mechanically stressed, favoring the unwrapping process. So, initially, the dissociating

DNA segment facilitates the unwrapping process for the adjacent DNA segment. According to the recent theoretical paper, saymmetric unwrapping of H3 nucleosomes rather than symmetric is an energetically more favorable process. Our data for CENP-A nucleosomes suggest that a similar model can also be applied to this type of nucleosome.

Overall, a variety of unique structural characteristics of canonical and centromere nucleosomes on the nanoscale have been found. We found that CENP-A nucleosomes are more stable than canonical nucleosomes regardless of their lower wrapping efficiency. Moreover, time-lapse experiments demonstrate that nucleosomes with ~100 bp of DNA wrapped are in a transient state with elevated stability. These findings suggest that the amount of DNA wrapped around the histone core is not the only factor defining the nucleosome stability; instead, other interactions between the histone cores and DNA contribute to the stability. The unwrapping process is highly asymmetric, and it was observed with both types of nucleosomes, revealing a novel property of nucleosome dynamics. Additionally, HS-AFM revealed higher stability of CENP-A nucleosomes compared with H3 nucleosomes, in which dissociation of the histone core occurs prior to H3 nucleosome dissociation. The histone core of CENP-A nucleosomes remains intact even after the dissociation of DNA, so the reassembly of the CENP-A nucleosomes is facilitated. This feature of CENP-A nucleosomes can be important for centromere dynamics during mitosis and chromatin replication.

# CONCLUSIONS

In summary, it was found that the monoH3 $_{\rm nuc}$  wrap 145  $\pm$  23 bp and the diH3 $_{\rm nuc}$  wrap 149  $\pm$  24 bp, which are in the expected 147 bp value range. The primary binding location of H3 $_{\rm nuc}$  is in the 601 sequence, with only three out of 202 binding to locations outside the 601 region. The monoCENP-A $_{\rm nuc}$  samples had a wrapping efficiency of 137  $\pm$  43 bp, while the dinucleosome assemblies had a wrapping efficiency of 130  $\pm$  20 bp. The mapping of CENP-A $_{\rm nuc}$  was completed on the same DNA construct as that for H3 $_{\rm nuc}$ , with 93% of the nucleosomes binding to the 601 sequence. The CENP-A $_{\rm nuc}$  assembly had an elevated affinity at the end of the DNA template, with a decrease to 92% binding to the specific sequence compared to 99% for H3 $_{\rm nuc}$ .

The CENP- $A_{nuc}$  samples, on average, had a longer dwell time than  $H3_{nuc}$ , which supports the statement of increased stability of CENP- $A_{nuc}$  compared to  $H3_{nuc}$ .

The unraveling process of DNA is a nongradual process. The unwrapping of DNA starts at approximately 150 bp with the octameric core splitting into H2A/H2B dimers and H3/H4 tetramer components. CENP- $A_{\text{nuc}}$  bound to the same DNA construct, shows stably wrapped nucleosomes, with spontaneous unwrapping resulting in a decreased wrapping of  $\sim 110$  bp. CENP- $A_{\text{nuc}}$  core particle is significantly more stable than H3<sub>nuc</sub>.

The unwrapping process for both nucleosomes has an intermediate step, where the nucleosome is stably unwrapped, lasting for many frames. The time to unwrap the nucleosome varies, with some events taking over three frames and others taking only 0.8 s.

#### ASSOCIATED CONTENT

# Supporting Information

The Supporting Information is available free of charge at https://pubs.acs.org/doi/10.1021/acs.biomac.3c01440.

Movie S1: High-speed AFM analysis (AVI)

Movie S2: HS-AFM analysis of H3<sub>nuc</sub> unwrapping (AVI)

Movie S3: HS-AFM analysis of H3<sub>nuc</sub> unwrapping (AVI)

Movie S4: HS-AFM video of H3<sub>nuc</sub> analyzed (AVI)

Movie S5: HS-AFM analysis of unwrapping (AVI)

Movie S6: HS-AFM analysis of CENP- $A_{nuc}$  unwrapping (AVI)

Movie S7: HS-AFM analysis of CENP- $A_{nuc}$  unwrapping (AVI)

Movie S8: HS-AFM video of CENP- $A_{nuc}$  analyzed (AVI)

Additional analysis of nucleosome location and wrapping for high-speed AFM movies (DOC) and raw high-speed AFM movies (Movies S1–S9) are provided (PDF)

## AUTHOR INFORMATION

# **Corresponding Author**

Yuri L. Lyubchenko — Department of Pharmaceutical Sciences, University of Nebraska Medical Center, Omaha, Nebraska 68198-6025, United States; orcid.org/0000-0001-9721-8302; Phone: +402-559-1971; Email: ylyubchenko@unmc.edu

#### **Authors**

Shaun Filliaux – Department of Pharmaceutical Sciences, University of Nebraska Medical Center, Omaha, Nebraska 68198-6025, United States

Zhiqiang Sun – Department of Pharmaceutical Sciences, University of Nebraska Medical Center, Omaha, Nebraska 68198-6025, United States

Complete contact information is available at: https://pubs.acs.org/10.1021/acs.biomac.3c01440

# **Author Contributions**

Conceptualization, Y.L.L.; methodology, S.F. and Z.S.; validation, S.F. and Z.S.; formal analysis, S.F.; investigation, S.F.; resources, Y.L.L.; writing—original draft preparation, S.F.; writing—review and editing, S.F.; visualization, S.F.; supervision, Y.L.L.; project administration, Y.L.L.; and funding acquisition, Y.L.L. All authors have read and agreed to the published version of the manuscript.

### Funding

This work was supported by grants to Y.L.L. from NSF (MCB 1515346 and MCB 2123637).

### Notes

The authors declare no competing financial interest.

## ACKNOWLEDGMENTS

We thank Dr. Lyubchenko lab members for useful insight. The table of contents/abstract graphic was created with Bio-Render.com.

# ABBREVIATIONS

3WJ, three-way junction; AFM, atomic force microscopy;  ${\rm H3}_{\rm nuc}$ ,  ${\rm H3}$  containing nucleosomes; CENP-A<sub>nuc</sub>, CENP-A containing nucleosomes

## REFERENCES

- (1) McGinty, R. K.; Tan, S. Nucleosome Structure and Function. *Chem. Rev.* **2015**, *115* (6), 2255–2273.
- (2) Onufriev, A. V.; Schiessel, H. The Nucleosome: From Structure to Function through Physics. *Curr. Opin. Struct. Biol.* **2019**, *56*, 119–130.
- (3) Zhou, K.; Gaullier, G.; Luger, K. Nucleosome Structure and Dynamics Are Coming of Age. *Nat. Struct. Mol. Biol.* **2019**, 26 (1), 3–13
- (4) Pan, Y. G.; Banerjee, S.; Zagorski, K.; Shlyakhtenko, L. S.; Kolomeisky, A. B.; Lyubchenko, Y. L. A Molecular Model of the Surface-Assisted Protein Aggregation Process. *Biophysics* **2018**, No. 415703.
- (5) Lyubchenko, Y. L. Atomic Force Microscopy Methods for DNA Analysis. In *Encyclopedia of Analytical Chemistry*; Meyers, R. A., Ed.; Wiley, 2019; 1–31.
- (6) Clapier, C. R.; Cairns, B. R. The Biology of Chromatin Remodeling Complexes. *Annu. Rev. Biochem.* **2009**, 78 (1), 273–304.
- (7) Becker, P. B.; Workman, J. L. Nucleosome Remodeling and Epigenetics. *Cold Spring Harb. Perspect. Biol.* **2013**, *5* (9), a017905—a017905.
- (8) Forties, R. A.; North, J. A.; Javaid, S.; Tabbaa, O. P.; Fishel, R.; Poirier, M. G.; Bundschuh, R. A Quantitative Model of Nucleosome Dynamics. *Nucleic Acids Res.* **2011**, *39* (19), 8306–8313.
- (9) Stormberg, T.; Stumme-Diers, M.; Lyubchenko, Y. L. Sequence-Dependent Nucleosome Nanoscale Structure Characterized by Atomic Force Microscopy. *FASEB J.* **2019**, 33 (10), 10916–10923.
- (10) Stormberg, T.; Vemulapalli, S.; Filliaux, S.; Lyubchenko, Y. L. Effect of Histone H4 Tail on Nucleosome Stability and Internucleosomal Interactions. *Sci. Rep.* **2021**, *11* (1), 24086.
- (11) Stormberg, T.; Lyubchenko, Y. L. The Sequence Dependent Nanoscale Structure of CENP-A Nucleosomes. *Int. J. Mol. Sci.* **2022**, 23 (19), 11385.
- (12) Sun, Z.; Stormberg, T.; Filliaux, S.; Lyubchenko, Y. L. Three-Way DNA Junction as an End Label for DNA in Atomic Force Microscopy Studies. *Int. J. Mol. Sci.* **2022**, 23 (19), 11404.
- (13) Wang, Y.; Stormberg, T.; Hashemi, M.; Kolomeisky, A. B.; Lyubchenko, Y. L. Beyond Sequence: Internucleosomal Interactions Dominate Array Assembly. *J. Phys. Chem. B* **2022**, *126* (51), 10813–10821.
- (14) Lancrey, A.; Joubert, A.; Duvernois-Berthet, E.; Routhier, E.; Raj, S.; Thierry, A.; Sigarteu, M.; Ponger, L.; Croquette, V.; Mozziconacci, J.; Boulé, J.-B. Nucleosome Positioning on Large Tandem DNA Repeats of the '601' Sequence Engineered in Saccharomyces Cerevisiae. *J. Mol. Biol.* 2022, 434 (7), No. 167497.
- (15) Cutter, A. R.; Hayes, J. J. A Brief Review of Nucleosome Structure. FEBS Lett. 2015, 589 (20PartA), 2914–2922.
- (16) McGhee, J. D.; Felsenfeld, G. Nucleosome Structure. Annu. Rev. Biochem. 1980, 49, 1115–1156.
- (17) Zhou, B.-R.; Yadav, K. N. S.; Borgnia, M.; Hong, J.; Cao, B.; Olins, A. L.; Olins, D. E.; Bai, Y.; Zhang, P. Atomic Resolution Cryo-EM Structure of a Native-like CENP-A Nucleosome Aided by an Antibody Fragment. *Nat. Commun.* **2019**, *10* (1), 2301.
- (18) Ohtomo, H.; Kurita, J.; Sakuraba, S.; Li, Z.; Arimura, Y.; Wakamori, M.; Tsunaka, Y.; Umehara, T.; Kurumizaka, H.; Kono, H.; Nishimura, Y. The N-Terminal Tails of Histones H2A and H2B Adopt Two Distinct Conformations in the Nucleosome with Contact and Reduced Contact to DNA. *J. Mol. Biol.* **2021**, 433 (15), No. 167110.
- (19) Luger, K. Crystal Structure of the Nucleosome Core Particle at 2.8 A° Resolution. *Nature* **1997**, 389, 251–260.
- (20) Park, P. J. ChIP-Seq: Advantages and Challenges of a Maturing Technology. *Nat. Rev. Genet.* **2009**, *10* (10), 669–680.
- (21) Poirier, M. G.; Oh, E.; Tims, H. S.; Widom, J. Dynamics and Function of Compact Nucleosome Arrays. *Nat. Struct. Mol. Biol.* **2009**, *16* (9), 938–944.
- (22) Szerlong, H. J.; Hansen, J. C. Nucleosome Distribution and Linker DNA: Connecting Nuclear Function to Dynamic Chromatin structureThis Paper Is One of a Selection of Papers Published in a

- Special Issue Entitled 31st Annual International Asilomar Chromatin and Chromosomes Conference, and Has Undergone the Journal's Usual Peer Review Process. *Biochem. Cell Biol.* **2011**, 89 (1), 24–34.
- (23) McKinley, K. L.; Cheeseman, I. M. The Molecular Basis for Centromere Identity and Function. *Nat. Rev. Mol. Cell Biol.* **2016**, *17* (1), 16–29.
- (24) Pidoux, A. L.; Allshire, R. C. The Role of Heterochromatin in Centromere Function. *Philos. Trans. R. Soc. B: Biol. Sci.* **2005**, 360, 569–579.
- (25) Stellfox, M. E.; Bailey, A. O.; Foltz, D. R. Putting CENP-A in Its Place. *Cell. Mol. Life Sci.* **2013**, *70* (3), 387–406.
- (26) Boopathi, R.; Danev, R.; Khoshouei, M.; Kale, S.; Nahata, S.; Ramos, L.; Angelov, D.; Dimitrov, S.; Hamiche, A.; Petosa, C.; Bednar, J. Phase-Plate Cryo-EM Structure of the Widom 601 CENP-A Nucleosome Core Particle Reveals Differential Flexibility of the DNA Ends. *Nucleic Acids Res.* **2020**, *48* (10), 5735–5748.
- (27) Sekulic, N.; Bassett, E. A.; Rogers, D. J.; Black, B. E. The Structure of (CENP-A-H4) 2 Reveals Physical Features That Mark Centromeres. *Nature* **2010**, *467* (7313), 347–351.
- (28) Stumme-Diers, M. P.; Banerjee, S.; Hashemi, M.; Sun, Z.; Lyubchenko, Y. L. Nanoscale Dynamics of Centromere Nucleosomes and the Critical Roles of CENP-A. *Nucleic Acids Res.* **2018**, *46* (1), 94–103.
- (29) Stumme-Diers, M. P.; Banerjee, S.; Sun, Z.; Lyubchenko, Y. L. Assembly of Centromere Chromatin for Characterization by High-Speed Time-Lapse Atomic Force Microscopy. In *Nanoscale Imaging*; Lyubchenko, Y. L., Ed.; Methods in Molecular Biology; Springer New York: New York, NY, 2018; 1814, 225–242.
- (30) Stumme-Diers, M. P.; Stormberg, T.; Sun, Z.; Lyubchenko, Y. L. Probing The Structure And Dynamics Of Nucleosomes Using Atomic Force Microscopy Imaging. *J. Vis. Exp.* **2019**, *143*, No. 58820.
- (31) Stormberg, T.; Filliaux, S.; Baughman, H. E. R.; Komives, E. A.; Lyubchenko, Y. L. Transcription Factor NF-kB Unravels Nucleosomes. *Biochim. Biophys. Acta Gen. Subj.* **2021**, *1865* (9), No. 129934.
- (32) Vemulapalli, S.; Hashemi, M.; Lyubchenko, Y. L. Site-Search Process for Synaptic Protein-Dna Complexes. *Int. J. Mol. Sci.* **2022**, 23 (1), 212.
- (33) Vemulapalli, S.; Hashemi, M.; Kolomeisky, A. B.; Lyubchenko, Y. L. DNA Looping Mediated by Site-Specific SfiI–DNA Interactions. *J. Phys. Chem. B* **2021**, *125* (18), 4645–4653.
- (34) Miyagi, A.; Ando, T.; Lyubchenko, Y. L. Dynamics of Nucleosomes Assessed with Time-Lapse High-Speed Atomic Force Microscopy. *Biochemistry* **2011**, *50* (37), 7901–7908.
- (35) Lowary, P. T.; Widom, J. Nucleosome Packaging and Nucleosome Positioning of Genomic DNA. *Proc. Natl. Acad. Sci. U. S. A.* 1997, 94, 1183–1188.
- (36) Widom, J. Role of DNA Sequence in Nucleosome Stability and Dynamics. Q. Rev. Biophys. 2001, 34 (3), 269–324.
- (37) Menshikova, I.; Menshikov, E.; Filenko, N.; Lyubchenko, Y. L. Nucleosomes Structure and Dynamics: Effect of CHAPS. *Int. J. Biochem. Mol. Biol.* **2021**, *2*, 129–137. www.ijbmb.org
- (38) Lyubchenko, Y. L. Direct AFM Visualization of the Nanoscale Dynamics of Biomolecular Complexes. *J. Phys. Appl. Phys.* **2018**, *51* (40), 403001.
- (39) Lyubchenko, Y. L.; Shlyakhtenko, L. S. Chromatin Imaging with Time-Lapse Atomic Force Microscopy. In *Chromatin Protocols*; Chellappan, S. P., Ed.; Methods in Molecular Biology; Springer New York: New York, NY, 2015; 1288, 27–42.
- (40) Lyubchenko, Y. L. Nanoscale Nucleosome Dynamics Assessed with Time-Lapse AFM. *Biophys. Rev.* **2014**, *6* (2), 181–190.
- (41) Lyubchenko, Y. L.; Shlyakhtenko, L. S.; Ando, T. Imaging of Nucleic Acids with Atomic Force Microscopy. *Methods* **2011**, *54* (2), 274–283.
- (42) Blower, M. D.; Sullivan, B. A.; Karpen, G. H. Conserved Organization of Centromeric Chromatin in Flies and Humans. *Dev. Cell* **2002**, *2* (3), 319–330.

- (43) Schalch, T.; Steiner, F. A. Structure of Centromere Chromatin: From Nucleosome to Chromosomal Architecture. *Chromosoma* **2017**, 126 (4), 443–455.
- (44) Black, B. E.; Bassett, E. A. The Histone Variant CENP-A and Centromere Specification. *Curr. Opin. Cell Biol.* **2008**, *20* (1), 91–100.
- (45) Takizawa, Y.; Ho, C.-H.; Tachiwana, H.; Matsunami, H.; Kobayashi, W.; Suzuki, M.; Arimura, Y.; Hori, T.; Fukagawa, T.; Ohi, M. D.; Wolf, M.; Kurumizaka, H. Cryo-EM Structures of Centromeric Tri-Nucleosomes Containing a Central CENP-A Nucleosome. *Structure* **2020**, *28* (1), 44–53.e4.
- (46) Rop, V. D.; Padeganeh, A.; Maddox, P. S. CENP-A: The Key Player behind Centromere Identity, Propagation, and Kinetochore Assembly. *Chromosoma* **2012**, *121* (6), 527–538.
- (47) Chua, E. Y. D.; Vasudevan, D.; Davey, G. E.; Wu, B.; Davey, C. A. The Mechanics behind DNA Sequence-Dependent Properties of the Nucleosome. *Nucleic Acids Res.* **2012**, *40* (13), 6338–6352.
- (48) Kixmoeller, K.; Allu, P. K.; Black, B. E. The Centromere Comes into Focus: From CENP-A Nucleosomes to Kinetochore Connections with the Spindle. *Open Biol.* **2020**, *10* (6), No. 200051.
- (49) Claudet, C.; Angelov, D.; Bouvet, P.; Dimitrov, S.; Bednar, J. Histone Octamer Instability under Single Molecule Experiment Conditions. *J. Biol. Chem.* **2005**, 280 (20), 19958–19965.
- (50) Bilokapic, S.; Strauss, M.; Halic, M. Histone Octamer Rearranges to Adapt to DNA Unwrapping. *Nat. Struct. Mol. Biol.* **2018**, 25 (1), 101–108.
- (51) Chen, Y.; Tokuda, J. M.; Topping, T.; Meisburger, S. P.; Pabit, S. A.; Gloss, L. M.; Pollack, L. Asymmetric Unwrapping of Nucleosomal DNA Propagates Asymmetric Opening and Dissociation of the Histone Core. *Proc. Natl. Acad. Sci. U. S. A.* **2017**, *114* (2), 334–339.
- (52) Onoa, B.; Díaz-Celis, C.; Cañari-Chumpitaz, C.; Lee, A.; Bustamante, C. Real-Time Multistep Asymmetrical Disassembly of Nucleosomes and Chromatosomes Visualized by High-Speed Atomic Force Microscopy. ACS Cent. Sci. 2024, 10 (1), 122–137.
- (53) Ngo, T. T. M.; Ha, T. Nucleosomes Undergo Slow Spontaneous Gaping. *Nucleic Acids Res.* **2015**, 43 (8), 3964–3971.
- (54) Zhang, B.; Zheng, W.; Papoian, G. A.; Wolynes, P. G. Exploring the Free Energy Landscape of Nucleosomes. *J. Am. Chem. Soc.* **2016**, 138 (26), 8126–8133.
- (55) Mondal, A.; Kolomeisky, A. B. Why Nucleosome Breathing Dynamics Is Asymmetric? *Biophys. J.* **2024**, *123* (3), 226A.